2020-1

Efficient Incorporation of Fatigue Damage Constraints in Wind Turbine Blade Optimization

Bryce Ingersoll
Brigham Young University

Andrew Ning
Brigham Young University, aning@byu.edu

ORIGINAL ARTICLE

Efficient Incorporation of Fatigue Damage Constraints in Wind Turbine Blade Optimization

Bryce Ingersoll, MS[1]* | **Andrew Ning, PhD**[1]*

[1]Brigham Young University, Provo, UT, 84604, U.S.A.

Correspondence
Bryce Ingersoll MS
BYU, CTB 435
Provo, UT, 84604
Email: bryceingersoll@byu.edu

Funding information
National Renewable Energy Laboratory

Wind turbine design is a challenging multidisciplinary optimization problem, where the aerodynamic shapes, structural member sizing, and material composition must all be determined and optimized. Some previous blade design methods incorporate static loading with an added safety factor to account for dynamic effects. Others incorporate dynamic loading, but in general limit the evaluation to a few design cases. By not fully incorporating the dynamic loading of the wind turbine, the final turbine blade design is either too conservative by overemphasizing the dynamic effects or infeasible by failing to adequately account for these effects. We propose an iterative method that estimates fatigue effects during the optimization process while quickly converging to the true solution. We also demonstrate an alternate approach where a surrogate model is trained to efficiently estimate the dynamic loading of the wind turbine in the design process. In contrast to the iterative method, there is significant upfront computational cost to construct the surrogate model. However, this surrogate model has been generalized to be used for different rated turbines, and for the scenarios studied in this paper can predict the fatigue damage of a wind turbine with less than 5% error. These methods can be used instead of the more computationally expensive method of calculating the dynamic loading of the turbine within the optimization routine.

KEYWORDS
wind turbine, blade design optimization, fatigue constraints, loading extrapolation, dimensional analysis, surrogate model

1 | BACKGROUND

An effective blade design optimization method can significantly increase the performance of a wind turbine. During the design process, the material composition, aerodynamic shapes, and sizing of the structural members must all be determined and optimized. This set of design variables define the aerodynamic and structural performance of the wind turbine, which factor into the wind turbine's cost of energy, or COE. The blade design must also satisfy a number of constraints to ensure safe operation in a series of design load cases [1, 2, 3], which cover the various conditions in which the wind turbine may operate.

To ensure that the wind turbine is able to safely operate in conditions specified by design load cases, structural constraints are specified during the design optimization process. These constraints include, but are not limited to, bounds on the strains experienced by the blade, clearance between the tower and blades, and fatigue. It is important in the blade design process to include fatigue damage constraints because the design life for wind turbines is often twenty or more years. Many wind turbine component designs, including the blade, are driven by constraints on the fatigue damage [4, 5, 6, 7].

The fatigue damage is determined from the dynamic loading experienced by the wind turbine. Calculating the dynamic loading requires performing an unsteady simulation and is thus computationally expensive compared to the rest of the design analysis [8]. This is especially true when the dynamic response of the wind turbine is calculated for an extensive set of design load cases. Bottasso et al. show that the computational time for a design routine that calculates a limited subset of all design load cases is on the order of one to two days [9]. Thus, the computational expense of running the dynamic simulations limits the number of design load cases that can be used in the blade design process.

To reduce the computational cost of the blade design routine, some studies neglect dynamic load constraints, and instead use static load conditions with an extra safety factor to estimate the impact of dynamic loads [10, 11, 12, 13]. Fatigue effects are not directly calculated, but are often accounted for by including a safety factor in the computed stresses and strains to estimate fatigue effects. While this is a cheap alternative to actually determining the fatigue damage, it is difficult to determine whether the safety factor is adequate or too conservative without actually calculating the wind turbine's damage equivalent loading.

The purpose of this work is to develop a method that determines the fatigue damage and extreme bending moments by evaluating the turbine's dynamic loading in the optimization routine that is not prohibitively computationally expensive if a large suite of design load cases are used. Such a method would allow for the efficient optimization of a more realistic blade design. The purpose of this work is to present two different approaches that accomplish these goals. As proposed but not demonstrated in our previous work [12, 14], the first approach involves calculating and updating equivalent fatigue damage along the blade by performing a dynamic simulation of the wind turbine outside of the optimization loop. This fatigue damage constrains the turbine blade design during its optimization routine. Once the optimization is complete, the fatigue damage of the final design is calculated, and the design is again optimized using the updated equivalent damage. We show that this iterative method converges to the true solution after four to five complete optimized designs are found and then subsequently used in the next optimization, and is much faster than including the evaluation of damage equivalent and extreme moments within the loop.

The method described in the previous paragraph is an improvement over evaluating the dynamic loading of the

wind turbine in the loop. However, there is a steep learning curve to implementing a dynamic evaluation code in a blade optimization framework. The second approach replaces the evaluation of the damage equivalent and extreme moments of the turbine with a surrogate model. Surrogate models have been used previously in wind turbine optimization. One surrogate optimization methodology implements a high-fidelity viscous-inviscid interaction code to evaluate the aerodynamic design [15]. Another approach using a Kriging fit to optimize the site-specific aerodynamic design [16]. Our approach is unique in that the surrogate model is used to predict the fatigue damage and extreme loads for a variety of design load cases and is implemented in a blade optimization routine. Developing the surrogate model for this specific use allows us to effectively develop a more broadly useful surrogate model that can be used in a number of different turbine design studies.

This surrogate model is trained using a variety of differently rated horizontal axis wind turbines. Once trained, the model is cheap to evaluate and estimates the equivalent fatigue damage, potentially even for turbines outside the training set. Once the initial work to create the surrogate model is done, there is no need to evaluate the dynamic loading within the optimization routine. Using a surrogate model will allow for quicker implementation of fatigue damage constraints in various conceptual studies in the blade design process.

2 | FORMULATION OF THE TURBINE BLADE DESIGN PROBLEM

To demonstrate our approach, we first define the blade optimization problem. We then describe the integration of the dynamic loading into the optimization routine. Finally, we describe necessary calculations used to convert the damage equivalent and extreme moments experienced by the turbine into optimization constraints.

The static portion of the blade analysis is done in RotorSE, an engineering model for analysis and optimization of horizontal axis wind turbines [17]. RotorSE is written within the OpenMDAO framework [18], an open-source platform that supports multidisciplinary analysis and optimization.

The objective of the blade optimization routine is minimize the wind turbine's cost of energy (COE), which is defined as [19]:

$$COE = \frac{OPEX(1-T) + FR(TCC + BOS)}{AEP} \tag{1}$$

where $OPEX$ is the overall project expenditures, T is the tax deduction rate on $OPEX$, FR is the financing rate, TCC is the turbine capital costs, and BOS is total balance of station costs. Specifically, a value of 0.4 is used for T and 0.095 for FR.

As done in our previous work [12, 14], we optimize the coupled aero-structural design of the wind turbine blade. Four groups of design variables are included: aeroelastic design variables of chord and twist distribution control points, and structural design variables of spar cap and trailing edge thickness. Four control points are used for each aeroelastic distribution and five control points for each structural distribution, for a total of 18 design variables. In our previous work, we included an additional design variable of the maximum chord length position along the blade. This variable affected the placement of the four chord control points. We simplified this by not including this additional design variable and instead fixed the positions of the chord control points at evenly spaced intervals from the root to the tip.

We use the same constraint groups as done in our earlier work [12, 14], with the additional fatigue constraints explained in the next section. The strain and buckling of the spar cap and trailing edge are constrained, as well as the fatigue damage effects at the same locations. The flapwise and edgewise frequencies are also constrained, as well as the rotor thrust at rated power. Finally, we limit the maximum tip deflection to avoid collision between a rotor blade and the

tower. We refer the reader to our previous work for further details of these design constraints.

2.1 | Incorporation of FAST Routine

To determine the dynamic response of the wind turbine, we use FAST [20], an aeroelastic computer-aided-engineering tool, to perform the dynamic simulation. To connect the wind turbine design defined in RotorSE, we used AeroelasticSE[1], a python-wrapper for the FAST executable. AeroelasticSE formats the wind turbine design specifications into the proper input files for use in FAST. We modified AeroelasticSE so that it would format the changing blade design within the optimization routine.

We used the design specifications of the NREL 5MW reference wind turbine [21] for blade optimization. We also used the WindPACT baseline turbine models [22]. These wind turbines have been specifically designed for use in studying the scaling of aerodynamic loads. For each baseline reference turbine, a FAST executable was built from source. Each executable was unique in that it specified the turbine's torque and pitch control routines. The NREL 5MW control routines were developed by Jonkman et al. [23], while the WindPACT reference turbines used a simple pitch control routine.

In the RotorSE framework, structural constraints are determined at specific radial positions, with an additional position at the root. For this study, we specified seventeen positions to calculate structural constraints along the length of the turbine blade. The first three point locations (as a fraction of the blade length) are 0.0222, 0067, 0.111. The fourth to the fourteenth blade locations are linearly spaced from 0.167 to 0.833. The last three points are located at 0.889, 0.933, and 0.978. FAST requires the user to specify at which locations loading data will be recorded. This is done by specifying the locations of the virtual strain-gages in FAST.

A limitation of FAST v7.0 is that only seven locations for virtual strain gages can be specified in a given simulation. Thus, bending and loading information can only be recorded at seven distinct points along the length of the blade, not including the blade root. If we desire to calculate the dynamic loading at each radial position specified in RotorSE, FAST must be run three times. Within FAST v8.0, the maximum number of virtual strain gages has been increased to nine, but we chose to use FAST v7.0 because some features and capabilities of v7.0 have not been implemented in v8.0.

To reduce the computational cost, we specified a subset of radial positions that would result in a small error between the interpolated and actual values at the seventeen radial positions used in RotorSE. We set this subset of radial positions to [1,3,5,7,9,12,17], and the corresponding blade fractions are previously described. An example of the interpolation can be seen in Figure 1. The root mean square difference between the calculated and interpolated data was $\sim 0.44\,\%$.

To evaluate the dynamic loading using FAST, we must specify the wind conditions during the simulation. These conditions were determined by a number of design load cases (DLCs), which have been specified by the IEC Design Standard for onshore wind turbines [1]. The purpose of these DLCs is to evaluate the turbine's response in a variety of wind conditions with respect to fatigue and ultimate strength analysis. To demonstrate this methodology, a selection of design load cases shown in Tables 1 and 2 were used in this study, though it is straightforward to add additional design cases. The included design load cases specify power production while the wind turbine experiences normal and extreme turbulence, extreme gusts and wind shear, as well as parked configurations with extreme yaw misalignment. The specific conditions were chosen because they have been show to most likely drive and affect the wind turbine design [24].

A given design load case is simulated using a set of wind input files. Non-turbulent wind files were generated using IECWind[2]. A short description and number of wind files generated for each non-turbulent DLC is in Table 1. Depending

[1] https://nwtc.nrel.gov/AeroelasticSE

[2] http://wind.nrel.gov/designcodes/preprocessors/IECWind

on the particular design load case, either a single wind input file is sufficient to fully simulate the intended environmental conditions (such as DLC 6.1 and 6.3), while others require multiple wind input files.

The turbulent wind files were generated using TurbSim[3]. Specifications used in TurbSim are listed in Table 3. For each average wind speed, six eleven minute wind files were created. To expedite the wind input file generation process, a python wrapper for TurbSim was created to quickly create and save the generated files. Table 2 gives a brief description of the design load cases simulated using the wind input files generated by TurbSim.

In the main input file for FAST, we specified the length of the simulation Tmax, integration time step DT, and the start of the recorded data TStart, and that it would be a time marching solution (using the FAST input AnalMode). We used different simulation times for the turbulent and non-turbulent wind input files; specifically the turbulent simulations were 640 seconds, and the non-turbulent simulations were 100 seconds. Also within the main input file, we specified what outputs from the simulation we wanted to record. We recorded the root bending moments in the edgewise and flapwise directions, as well as the bending moments at the specified radial positions. These specifications are listed in Table 4.

2.2 | Fatigue Calculation

To determine the blade fatigue, we first calculated damage equivalent moments (DEM) from the simulation data. The cycle ranges and peaks of each simulation are recorded in a rainflow routine. The formula for a damage equivalent moment (DEM) is derived in MLife[4]:

$$DEM = \left(\frac{\sum_i [n_i (L_i)^m]}{n^{ST}} \right)^m \tag{2}$$

where L_i is the load range for the ith cycle, m is the Wholer exponent, n^{ST} is the equivalent number of counts for the time series, and n_i is the specific cycle value (0.5 for a half count and 1.0 for a full count). The recorded data from the rainflow routine is used in equation 2 to calculate the DEMs. This is done for the edgewise damage equivalent moments DEM_x and flapwise damage equivalent moments DEM_y.

Once the edgewise and flapwise damage equivalent moments are determined, they are transferred to the elastic center and principal axes of the blade section. We then calculate the edgewise strain ϵ_U and flapwise strain ϵ_L, where

$$\epsilon_U = -\left(\frac{DEM_1}{EI_{11}} y_U - \frac{DEM_2}{EI_{22}} x_U + \frac{F_z}{EA} \right) \tag{3}$$

and

$$\epsilon_L = -\left(\frac{DEM_1}{EI_{22}} y_L - \frac{DEM_2}{EI_{22}} x_L + \frac{F_z}{EA} \right) \tag{4}$$

The stiffnesses EI, cross sectional areas A, distances x and y and Young's modulus E are determined in the RotorSE framework. The number of cycles to failure in the edgewise direction N_{fU} and number of cycles to failure in the flapwise direction N_{fL} are defined as

$$N_{fU} = \left(\frac{\epsilon_{max}}{\eta \epsilon_U} \right)^m \tag{5}$$

[3] https://nwtc.nrel.gov/TurbSim

[4] https://nwtc.nrel.gov/MLife

and

$$N_{fL} = \left(\frac{\epsilon_{max}}{\eta \epsilon_L}\right)^m \tag{6}$$

where ϵ_{max} is the ultimate strain, η is the material safety factor (a value of 1.3 was used), and m is the Wöhler exponent (typically 10 for composite materials that are glass-reinforced [25]). Once the number of cycles to failure has been calculated, we determine the equivalent damage in the edgewise and flapwise direction, or

$$\text{damage}_U = \frac{N}{N_{fU}} \tag{7}$$

and

$$\text{damage}_L = \frac{N}{N_{fL}} \tag{8}$$

where N is the planned lifetime number of cycles. For this study, we used a design life of 20 years. A calculated damage greater than 1 corresponds to failure due to fatigue.

2.3 | Extreme Moment Extrapolation

From the simulated dynamic response, the peaks can be determined and visualized as a distribution (see the histogram in Figure 2). As defined by the IEC Design Standard for onshore wind turbines [1], an extreme moment should be extrapolated from the calculated peak distribution and then used to constrain the blade design. We fit a Gaussian distribution to the loading data (see the fit in Figure 2) and use this to estimate the extrapolated loads [26]. The probability density P for a Gaussian distribution is defined as:

$$P(F) = \frac{1}{\sqrt{2\pi\sigma^2}} e^{-\frac{(F-\mu)^2}{2\sigma^2}} \tag{9}$$

where μ is the mean, σ is the standard deviation, and F is the extreme load. For a given 10 minute simulation, the IEC Design Standard specifies that the extreme event F should have a probability P of 3.8×10^{-7}. Equation 9 was used to determine the extreme extrapolated moment. We calculated the extrapolated bending moment at the blade root, as well as along the length of the blade in both the edgewise and flapwise directions. The extreme moments were incorporated as constraints in the blade design process by using them to calculate the maximum strain in the upper and lower sections of the spar cap and trailing edge, where

$$\epsilon_U = -\left(\frac{M_{e,x}}{EI_{11}} y_U - \frac{M_{e,y}}{EI_{22}} x_U + \frac{F_z}{EA}\right) \tag{10}$$

and

$$\epsilon_L = -\left(\frac{M_{e,x}}{EI_{22}} y_L - \frac{M_{e,y}}{EI_{22}} x_L + \frac{F_z}{EA}\right) \tag{11}$$

The calculated strain is then constrained by the ultimate strain (a value of 10^{-2} was used for the spar cap, and 0.5×10^{-2} for the trailing edge).

3 | INCORPORATION OF FATIGUE DAMAGE CONSTRAINTS

As described in the previous section, the routine to determine the dynamic loading of the wind turbine using FAST provides useful data that can be incorporated into the wind turbine blade optimization process. The calculated damage equivalent moments and extreme extrapolated events from this routine can be incorporated into design constraints that drive the design. Because of the higher-fidelity of the method used to calculate these constraints, the accuracy of the overall design process is improved and the final design is more realistic.

Unfortunately, the computational cost to evaluate the wind turbine's dynamic loading using FAST within the optimization routine is prohibitively expensive. The sequential evaluation of the blade design using all the prescribed input wind files (132 in total) varies depending on the machine being used, but can be on the order of two hours. Within a single optimization, this routine is run several hundred or even thousands of times. The computation time is lessened when we parallelize this calculation, but a full optimization routine may take several days or weeks to complete, or potentially months if calculated sequentially.

3.1 | Fixed DEM Iterative Method

The prohibitively expensive cost of performing a dynamic simulation led us to explore methods where the blade optimization process could be improved without running the simulation inside the design loo. As proposed but not tested in our previous work [12, 14], the first proposed approach involves calculating and updating the damage equivalent and extreme moments along the blade outside the optimization routine. We freeze the damage equivalent and extreme moments during the initial turbine blade optimization. We theorize that while the calculated damage and stresses will have a first order change with the blade design, the calculated loading will change less significantly, and it will suffice to update the loading only periodically. Once the optimization is complete, the damage equivalent and extreme moments of the final design are calculated, and the design is again optimized using the updated damage equivalent and extreme moments. We show that this iterative method converges within four or five complete optimizations to a solution similar to calculating the dynamic loading within the loop.

To begin, initial values for the design variables are chosen. We evaluate the dynamic loading using FAST for the wind input files listed in the previous section. Within this routine, the damage equivalent moments in the edgewise and flapwise directions are calculated, as well as the extreme extrapolated moments. This is computed for all wind input files (132 in total). The individual runs are not dependent on each other, so this process can be parallelized and completed in several minutes.

Once the dynamic loading of the wind turbine has been evaluated, we compare the edgewise and flapwise DEM values, as well as the extreme moments, determined from using the different wind input files at each virtual strain gage position. The maximum damage equivalent and extreme moments at each position can then be used in the fatigue and strain constraints in the blade optimization routine.

We then optimize the wind turbine blade to determine an improved blade design. Once the initial optimization is complete, we perform a dynamic simulation of the new wind turbine to calculate new DEMs and extreme moments based on the updated design. The blade design is re-optimized with the updated loading. We repeat this process until there is a small change in the objective value (less than 0.01%), COE. In summary, the iterative method follows this procedure:

1. Choose initial turbine blade design
2. Calculate DEMs and extreme moments using all wind input files

3. Determine maximum DEMs & extreme moments
4. Optimize with pre-calculated dynamic loading for use in strain and fatigue constraints
5. Set optimized design as new initial design
6. Repeat steps 2-5 until convergence

As can be seen in Figure 3, this method modifies the blade design and the wind turbine's COE in each successive complete optimization. In fact, after each optimization is complete, the calculated damage equivalent moments are higher than the previous calculated values, due to a slimmer blade. This can be seen when observing the chord spline in Figure 4. The twist distribution is also shown. We also include an optimized blade design when static loading with an additional safety factor of 1.35 to account for dynamic effects is used to constrain the blade design, as done in our previous work [12].

We note that when static loading with a safety factor to account for dynamic effects is used to constrain the blade design, the resulting COE is much lower (see Figure 3). When the fatigue damage using dynamic loading is calculated for this blade design, fatigue constraints are violated at the root of the blade. The corresponding damage will lead to design in failure in about 11.1 years (where the assumed design life is 20 years), making the blade design as a whole infeasible. Thus, the fatigue damage constraints have a significant effect on the design.

We completed a blade optimization where the damage equivalent moments and extreme moments are determined within the optimization loop for a subset of active wind input files. This result is shown in Figure 3. The dynamic loading of the wind turbine was evaluated at all wind files at the final design, and was found to not violate any constraints.

While using a subset of wind input files for the dynamic in-the-loop blade optimization worked for this specific wind turbine, that most likely will not be the usual case. If the final design violated constraints determined from design load cases not included in the optimization, the optimization would need to be redone. We needed to know what specific wind input files drive the blade design, and only determined this by completing the iterative fixed-DEM blade optimization method. Finally, this optimization took on the order of two days to complete, where the fixed-DEM method took about five hours. While updating the effective fatigue damage is quite involved, the iterative approach is less computationally expensive than including the evaluation of the dynamic loading in the loop. In this case of optimizing the NREL 5MW reference turbine, we only needed to determine the dynamic loading four times. The fifth optimization showed that the method had converged.

3.2 | Surrogate Replacement for Dynamic Simulation

The iterative method explained in the previous section significantly reduces the computational cost of incorporating the dynamic loading of the wind turbine in its blade optimization routine. However, there is still significant work that must be done to incorporate a dynamic code outside of the optimization routine. The wind input files for the wind turbine to be optimized must be generated as done in section 2.1. The pitch and torque control routines must also be specified for the wind turbine, as well as the turbine specifications used in FAST. In addition, we still must evaluate the dynamic loading several times in the optimization to find an optimal design.

We have implemented a surrogate model that estimates the dynamic loading on the wind turbine. This has the benefit of incorporating the dynamic loading of the wind turbine without subsequent users needing to have any familiarity with FAST or a dynamic code. There is a sizable upfront cost to calculate the necessary data to train the surrogate model, and the person that generates the surrogate model data needs to know how to use FAST or a similar dynamic code. However, by doing a proper dimensional analysis of the input and output parameters of the model, the calculated data can be generalized and used in the optimization of a wind turbine at various different conditions,

including wind turbines of different power ratings.

The dynamic simulation of a wind turbine using FAST and other routines produces a huge variety and depth of information. Some examples include output data related to nacelle yaw, platform and rotor-furl motions, tower, shaft, and hub loading, as well as generator and HSS information, all of which are calculated in this routine. For our purpose, though, we are only interested in the DEMs determined from the FAST-calculated moments along the length of the blade, as well as the extreme extrapolated moments M_e. These outputs are chosen because they are used to define constraints in the blade optimization problem, and are dependent on aspects of the blade design as well as the wind input files used in FAST. We can define these relationships as g and h, where

$$DEM = g(\text{blade design, wind input files}) \tag{12}$$

$$M_e = h(\text{blade design, wind input files}) \tag{13}$$

Not all aspects of the blade design and wind input files significantly affect the damage equivalent and extreme moments. We determined which aspects most affect these values by varying each specific design aspect x_i used in FAST. Each aspect was increased and then decreased by 10% from its nominal value. If varying x_i either way created more than a 3% relative difference with respect to the damage equivalent and extreme moments calculated using the baseline configuration, we chose to include it in g and h. We chose a high threshold to determine what design aspects would be included to reduce the complexity of the surrogate model.

From this analysis, we determined the blade design aspects that most significantly affected the damage equivalent and extreme bending moments. For the reference wind turbines described in Section 2.1, these design aspects include the blade length r, chord distribution c, twist distribution θ, and rated torque Q. If the same set of design load cases are used, the turbulence intensity I_T used to generate the wind input files also affects the damage equivalent and extreme bending moments. Additional blade design aspects affected damage equivalent and extreme bending moment, such as the blade mass density. However, they were not as significant as the design aspects used in this analysis.

We can then rewrite equations 12 and 13 as

$$DEM = g(c, r, \theta, Q, I_T) \tag{14}$$

$$M_e = h(c, r, \theta, Q, I_T) \tag{15}$$

Using the Buckingham Pi theorem, we can rearrange equations 14 and 15 into non-dimensional Π groups by inspecting the units of each term. By inspection, we can determine non-dimensional Π groups. These groups can be

rearranged from equation 14 as

$$\Pi_1 = G(\Pi_2, \Pi_3, \Pi_4), \text{ where}$$
$$\Pi_1 = \frac{DEM}{Q} = \overline{DEM}$$
$$\Pi_2 = \frac{c}{r} = \overline{c}$$
$$\Pi_3 = \theta$$
$$\Pi_4 = I_T$$

Note that a new function G is used to relate the non-dimensional groups. A similar function H can be created for the extrapolated moments. The non-dimensional groups are exactly the same except for the first group, where M_e replaces DEM. The first Π group for both functions were set as the outputs of our surrogate model, and are listed in Table 5. The second, third and fourth Π groups are set as the inputs of our surrogate model, and are listed in Table 6.

We used Latin hypercube sampling (LHS) to choose training points from the design space. LHS uses a stratified sampling scheme to improve on the coverage of a given input space. As noted in other works [27, 28], LHS reduces random sampling error, while requiring a similar amount of resources.

After becoming familiar with this optimization problem, we can further restrict the domains of the chord and twist distributions. By doing so, more points are trained where the optimization will likely drive the design. This will also improve the accuracy of the surrogate model. An example of this is shown in Figure 5, where each control point of the chord and twist distributions is a given more restrictive bounds.

Once the selected points are trained, a cheap-to-evaluate function is created. A number of different function types can be used, such as a least squares approximation or a polynomial fit. In this work, we used the surrogate modeling toolbox[5] which provides a number of different fit types. Specifically, we incorporated a least squares, 2nd order polynomial, radial basis function, Kriging, Kriging partial least squares (KPLS), and a KPLS-kernel (KPLSK) method. As part of the construction of the surrogate model, we compared the accuracy of each of these fits.

We determined the accuracy of the surrogate model and the appropriateness of the fit type with k-fold cross validation. A 5-fold cross-validation is used, where the points are grouped into five folds. One fold is removed from the training portion of the surrogate model. Once the surrogate model has been trained, the points of the left-out fold are used to validate the created surrogate model. Specifically, the error between the predicted values and the actual values of the left-out points is calculated. The root mean square (RMS) of these errors is then determined. This is then repeated for all folds, and the root mean square of all errors is then calculated. This results in a single error value, which can be compared to other error values using different fit types and number of training points.

The overall RMS error was calculated and compared using various fits and number of training points, as shown in Figure 6. The Kriging, Kriging partial least squares (KPLS), and KPLS-kernel (KPLSK) method generally resulted in similar error values ($\sim 3.06\%$), where the 2nd order polynomial, radial basis function and least squares fits resulted in higher errors ($\sim 3.52 - 6.83\%$). Therefore, we used a Kriging fit because it took less time to construct than the KPLS and PKLSK methods. We show resulting error values when the number of training points is varied in the following section.

To test the number of training points needed for the surrogate model, we trained it using the WindPACT reference turbines [22]. The turbine ratings for the WindPACT reference turbines were 750 kW, 1.5 MW, 3.0 MW, and 5.0 MW. Once we had calculated the points and trained the surrogate model using the data from all four wind turbines, we performed a 5-fold cross validation using various number of training points. The resulting root mean square error is

[5] https://smt.readthedocs.io/en/latest/

shown in Figure 7. As expected, as the number of training points increases, the error of the model decreases. Also, using more than 1000 points for each turbine configuration does not significantly increase the surrogate model accuracy, so we chose to train 1000 points for each turbine configuration. While the computational cost is significant, each calculation is independent of each other and be done in parallel, and the total data set can be calculated in a few hours.

3.3 | Surrogate Model Results

The trained surrogate model can often reasonably predict the fatigue damage for a wind turbine that has not been used to in the training of the model. We tested this by training a surrogate model with the 1.5 and 5.0 MW WindPACT reference turbines using the loading conditions described in section 2.1. We next calculated the damage equivalent moments using FAST for the 3.0 MW WindPACT reference turbine. Once the dynamic loading had been evaluated, we compared the estimated damage from the surrogate model with the FAST calculated damage. This is shown in Figure 8. The surrogate model predicts the equivalent fatigue damage of the 3.0 MW WindPACT reference turbine with a root mean square error of 1.15 %. While the surrogate model also predicts extreme loads, only fatigue damage results are included since they often drive the design.

In addition, we wanted to determine how well the surrogate model could predict the fatigue damage for a wind turbine that not only was not used to train the model, but also was not in the range of rated power of wind turbines used to train the model. We did this by training the surrogate model using the 1.5 MW, 3.0 MW, and 5.0 MW WindPACT reference turbines using the loading conditions described in section 2.1. We next calculated the damage equivalent moments using FAST for the 0.75 MW reference turbine. Once the dynamic loading had been evaluated, we compared the estimated damage from the surrogate model with the FAST calculated damage. This is shown in Figure 9. The surrogate model predicts the equivalent fatigue damage of the 0.75 MW WindPACT reference turbine with a root mean square error of 4.77 %.

The third cross validation of the surrogate model was to train the model using the four WindPACT reference turbines to predict the fatigue damage of the NREL 5 MW reference turbine. The NREL 5 MW turbine differs from the WindPACT 5.0 MW reference turbine with different nacelle, hub and generator properties, as well as the group of airfoils used to define the blade cross section. The results are shown in Figure 10. As can be seen in Figure 10a, the surrogate model over-predicts the fatigue damage in the edgewise direction, and as seen in Figure 10b, the surrogate model under-predicts the fatigue damage in the flapwise direction, with an overall root mean square error of 4.4 %.

Once we had cross validated the surrogate model, we tested the surrogate model within the optimization loop. Note that it is important to impose design variable limits so that the surrogate model does not extrapolate values not included in the training of the surrogate model. The NREL 5MW reference turbine was used. The optimized objective (COE) was 6.229 cents/kWh, and the final aerodynamic design is shown in Figure 11. The final design was similar to the design determined using the iterative fixed-damage method. The computation time was on par with one full optimization of iterative method, which shows that if we don't consider the upfront cost to train the surrogate model, this method is quite efficient in incorporating the wind turbine's dynamic response within the optimization loop.

4 | CONCLUSIONS & FUTURE WORK

As shown using the iterative method, we were able to incorporate extreme moments and fatigue effects determined using the wind turbine's dynamic loading without having to necessarily calculate it inside the optimization loop. Within four to five design optimizations, the fixed-DEM method was able to determine a much improved blade design. This

design had a similar COE compared to the COE of the optimized design when calculating the dynamic loading of the wind turbine within the optimization loop (see Table 7). This method is considerably less expensive than evaluating the dynamic loading of the wind turbine within the loop. While we demonstrated the iterative method using a subset of all design load cases, the computational cost does not significantly increase when additional wind input files are included. This is because this computation is done outside of the optimization loop.

We developed a surrogate model that can be used to estimate the damage equivalent and extreme bending moments experienced by a wind turbine. As an extensive set of training data is built up, its use for additional turbines can be increased. Training data for specific studies can be also determined and used when we want to quickly estimate the dynamic loading for a given turbine.

Using a surrogate model to estimate the damage equivalent and extreme moments separates the work needed to calculate the dynamic loading with different studies that can be done to improve the efficiency of wind turbines. Once the dynamic loading has been generated, the surrogate model can be trained and used for a variety of different conceptual studies. There is a trade-off in a loss in accuracy when using the surrogate model. The studies in this paper showed a 5% RMS error in the estimated damage equivalent and extreme moments.

However, we showed that using a surrogate model results in an improved design with significantly less computational cost than including the evaluation of the dynamic loading within the loop. Once the upfront calculation for the training of surrogate model is complete, the optimization method is quite efficient, where the computation time was on par with one of the fixed-DEM method. Comparative information for the developed methods in listed in Table 7. Note that the error in the dynamic loading using the iterative method varies during the optimization process, and progressively becomes smaller as more optimized design loops are completed.

Future studies can continue to contribute to the data set used to estimate the damage equivalent and extreme moments. The current data set is contained in an open-source repository[6]. Future work could also continue to improve our methods that efficiently include the dynamic loading of a wind turbine within the blade design routine. For example, we used a simple Gaussian fit for the simulated loading data to extrapolate extreme events. Calculating a consistent extreme event-extrapolation can be very difficult. Both Ragan [29] and Lott [30] discuss some of these problems, such as when data outliers must be accounted for and what statistical fit is appropriate for the collected data. More complex methods could be incorporated to better estimate the extrapolated loads in future work.

In addition, the integration of the surrogate model to estimate fatigue damage constraints could be improved by increasing the complexity and fidelity of the surrogate model. For this study, we desired to limit the complexity of the surrogate model and used a high threshold value when determining what design aspects to include. This value could be lowered to include additional design aspects and increase the accuracy of the surrogate model, such as including the blade stiffness and mass density distributions. This increased fidelity has the potential to make the surrogate model more universal in its use in wind turbine blade design optimization.

REFERENCES

[1] IEC. Wind turbines Part 1: Design requirements, IEC 61400-1, 3rd edition. International Electrotechnical Commission (IEC) 2005;.

[2] Kong C, Bang J, Sugiyama Y. Structural Investigation of Composite Wind Turbine Blade considering Various Load Cases and Fatigue Life. Energy 2005;30(11-12):2101–2114.

[3] Manwell JF, McGowan JG, Rogers AL. Wind Energy Explained: Theory, Design and Application. John Wiley & Sons; 2010.

[6] https://github.com/byuflowlab/blade-damage

[4] Schubel P, Crossley R. Wind Turbine Blade Design. Energies 2012;5(9):3425–3449. http://www.mdpi.com/1996-1073/5/9/3425.

[5] Lee HG, Park J. Static Test Until Structural Collapse After Fatigue Testing of a Full-Scale Wind Turbine Blade. Composite Structures 2016;136:251–257.

[6] Bazilevs Y, Korobenko A, Deng X, Yan J. Fluid-Structure Interaction Modeling for Fatigue Damage Prediction in Full-Scale Wind Turbine Blades. Journal of Applied Mechanics 2016;83(6):061010.

[7] Meng H, Lien FS, Li L. Elastic Actuator Line Modeling for Wake-Induced Fatigue Analysis of Horizontal Axis Wind Turbine Blade. Renewable Energy 2018;116:423–437.

[8] Bottasso CL, Croce A, Sartori L, Grasso F. Free-Form Design of Rotor Blades. Journal of Physics Conference Series 2014 Jun;524(1):12–41.

[9] Bottasso CL, Campagnolo F, Croce A. Multi-disciplinary constrained optimization of wind turbines. Multibody System Dynamics 2012;27(1):21–53. http://dx.doi.org/10.1007/s11044-011-9271-x.

[10] Caboni M, Campobasso MS, Minisci E. Wind Turbine Design Optimization under Environmental Uncertainty. Journal of Engineering for Gas Turbines and Power 2016;138(8):082601.

[11] Barrett R, Ning A. Comparison of Airfoil Precomputational Analysis Methods for Optimization of Wind Turbine Blades. IEEE Transactions on Sustainable Energy 2016 Jul;7(3):1081–1088.

[12] Ning A, Damiani R, Moriarty P. Objectives and Constraints for Wind Turbine Optimization. Journal of Solar Energy Engineering 2014 06;136(4):041010–041010. http://dx.doi.org/10.1115/1.4027693.

[13] Kenway G, Martins J. In: Aerostructural Shape Optimization of Wind Turbine Blades Considering Site-Specific Winds American Institute of Aeronautics and Astronautics; 2008. http://dx.doi.org/10.2514/6.2008-6025.

[14] Ning A, Petch D. Integrated Design of Downwind Land-Based Wind Turbines using Analytic Gradients. Wind Energy 2016;19(12):2137–2152. http://dx.doi.org/10.1002/we.1972, we.1972.

[15] Sessarego M, Ramos-García N, Hua Y, Shen WZ. Aerodynamic Wind-Turbine Rotor Design using Surrogate Modeling and Three-Dimensional Viscous–Inviscid Interaction Technique. Renewable Energy 2016 03;93.

[16] Carrasco ADV, Valles-Rosales DJ, Mendez LC, Rodriguez MI. A Site-Specific Design of a Fixed-Pitch Fixed-Speed Wind Turbine Blade for Energy Optimization using Surrogate Models. Renewable Energy 2016;88:112 – 119. http://www.sciencedirect.com/science/article/pii/S0960148115304365.

[17] Ning A. RotorSE. National Renewable Energy Laboratory (NREL), Golden, CO (United States); 2013.

[18] Gray J, Moore K, Naylor B. OpenMDAO: An Open Source Framework for Multidisciplinary Analysis and Optimization. In: 13th AIAA/ISSMO Multidisciplinary Analysis Optimization Conference; 2010. p. 9101.

[19] Ning A, Dykes K. Understanding the Benefits and Limitations of Increasing Maximum Rotor Tip Speed for Utility-Scale Wind Turbines. Journal of Physics: Conference Series 2014;524(1):012087. http://stacks.iop.org/1742-6596/524/i=1/a=012087.

[20] Jonkman J, Buhl M. FAST User's Guide. NREL/EL-500e38230 2005;.

[21] Jonkman J, Butterfield S, Musial W, Scott G. Definition of a 5-MW Reference Wind Turbine for Offshore System Development. National Renewable Energy Laboratory (NREL) 2009 2;.

[22] Dykes K, Rinker J. WindPACT Reference Wind Turbines. National Renewable Energy Lab.(NREL), Golden, CO (United States);.

[23] Jonkman J. Offshore Code Comparison Collaboration (OC3) for IEA Task 23 Offshore Wind Technology and Deployment Offshore Code Comparison Collaboration (OC3) for IEA Task 23 Offshore Wind Technology and Deployment. NREL, Golden, CO 2010;.

[24] Resor B. Definition of a 5MW/61.5 m Wind Turbine Blade Reference Model. Albuquerque, New Mexico, USA, Sandia National Laboratories, SAND2013-2569 2013 2013;.

[25] Mandell JF, Samborsky DD. DOE/MSU composite material fatigue database: test methods, materials, and analysis. Sandia National Labs., Albuquerque, NM (United States); 1997.

[26] Madsen P, Pierce K, Buhl M. Predicting Ultimate Loads for Wind Turbine Design. National Renewable Energy Lab., Golden, CO (US); 1998.

[27] Iman R. Latin Hypercube Sampling. Wiley StatsRef: Statistics Reference Online 2008;.

[28] Stein M. Large Sample Properties of Simulations using Latin Hypercube Sampling. Technometrics 1987;29(2):143–151.

[29] Ragan P, Manuel L. In: Statistical Extrapolation Methods for Estimating Wind Turbine Extreme Loads American Institute of Aeronautics and Astronautics; 2007. https://doi.org/10.2514/6.2007-1221.

[30] Lott S, Cheng PW. Load Extrapolations Based on Measurements from an Offshore Wind Turbine at Alpha Ventus. Journal of Physics: Conference Series 2016;753(7):072004. http://stacks.iop.org/1742-6596/753/i=7/a=072004.

TABLE 1 Design load cases using non-turbulent wind files.

DLC	Description	Number of Wind Files
DLC 1.4 (ECD)	Evaluation of ultimate loads during regular power production with an extreme coherence gust with change in wind direction	6
DLC 1.5 (EWS)	Evaluation of ultimate loads evaluation during regular power production with the presence of extreme wind shear	4
DLC 6.1 (EWM50)	Evaluation of ultimate loads while in a parked configuration during a 50-year extreme steady wind event	1
DLC 6.3 (EWM01)	Evaluation of ultimate loads while in a parked configuration during a 1-year extreme steady wind event with extreme yaw	1

TABLE 2 Design load cases using turbulent wind files.

DLC	Description	Number of Wind Files
DLC 1.2 (NTM)	Evaluation of fatigue damage during normal power production in normal turbulence	60
DLC 1.3 (ETM)	Evaluation of ultimate loads during normal power production in extreme turbulence	60

TABLE 3 Specifications used when generating wind files.

Parameter	Value
V_{in}	3 m/s
V_{out}	25 m/s
V_{rated}	11.4 m/s
Average wind speeds for turbulent simulations	5, 7, 9, 11, 13, 15, 17, 19, 21, 23 m/s
Turbulence Model	Kaimal
IEC Class	I
Turbulence Class	B

TABLE 4 Specifications used in FAST simulations.

FAST Parameter	Value
Tmax	640.0 / 100.0 s
DT	0.0125 s
TStart	20.0 s
AnalMode	1
OutList	RootMxb1
	RootMyb1
	Spn[1-7]MLxb1
	Spn[1-7]MLyb1

TABLE 5 Outputs included in the surrogate model.

Name	Description	Number of Values
$\overline{DEM_y}$	DEMs in flapwise direction divided by Q	18
$\overline{DEM_x}$	DEMs in edgewise direction divided by Q	18
$\overline{M_{e,y}}$	extreme moments in flapwise direction divided by Q	18
$\overline{M_{e,x}}$	extreme moments in edgewise direction divided by Q	18

TABLE 6 Inputs used to train the surrogate model.

Name	Description	Num. of Values
I_T	IEC turbulence intensity value	1
$\overline{c}$	Non-dimensional chord distribution	4
θ_d	Twist distribution	4

TABLE 7 Comparison of developed methods to include dynamic loading in wind turbine blade design optimization. Note that the error listed is with respect to the dynamic loading calculated using FAST.

Method	Opt. Time	DLCs used	Opt. COE ($ / kWh)	Error in Dyn. Loading
In-the-loop	~ 2 days	select few	0.062379	exact
Iterative	~ 5 hours	full set	0.062374	<1%
Surrogate	~ 1 hour	full set	0.062287	~ 5 %

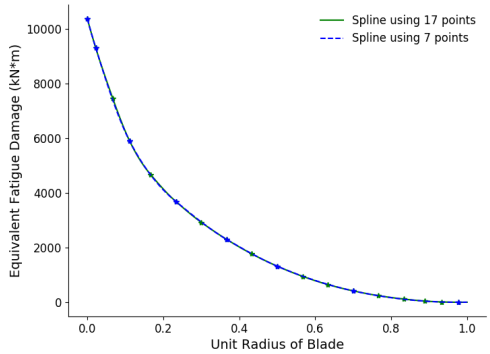

FIGURE 1 A comparison of calculated flapwise damage equivalent moments where virtual strain gages are placed at every radial position used in RotorSE (green) and where virtual strain gages are placed at a subset of all radial positions (blue).

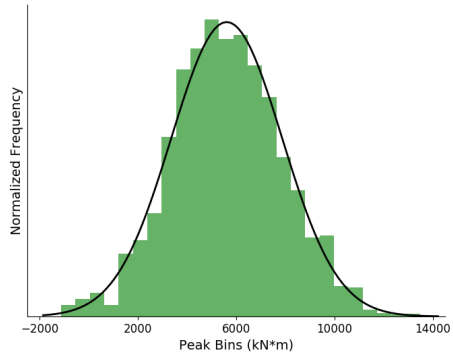

FIGURE 2 The bending moment distribution (green) at the blade root in the flapwise direction for a turbulent wind file. A Gaussian distribution (black) is fit to the data.

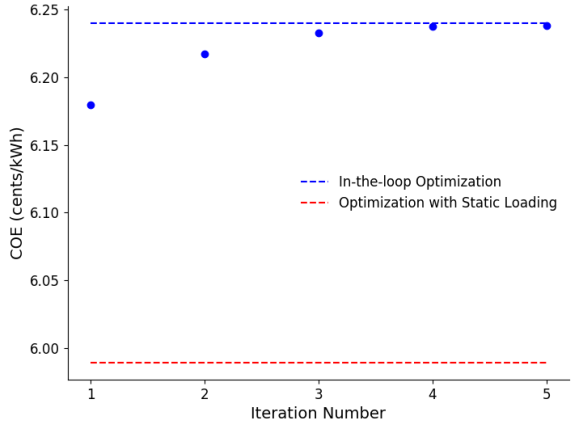

FIGURE 3 The cost of energy (COE) of the optimized design at the end of each optimization. By the fifth optimization, there is negligible change in the COE. The dashed blue represents the optimized result using the design determined by evaluating the dynamic loading within the loop. The red line represents the optimized COE when static loading is implemented.

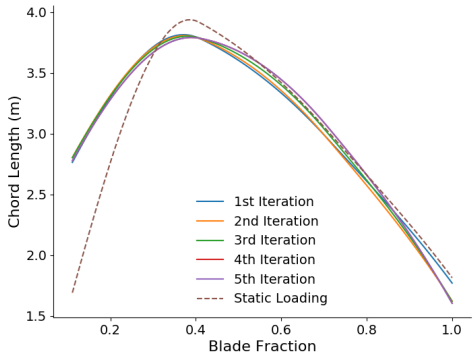

(a) Optimized chord splines

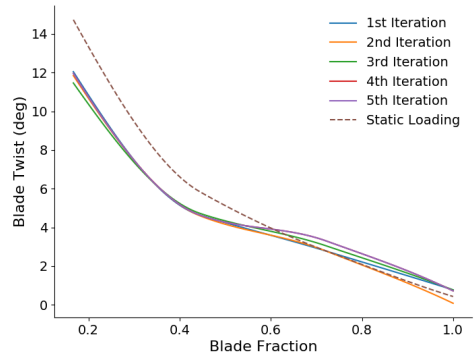

(b) Optimized twist splines

FIGURE 4 The optimized chord and twist splines at the end of each optimization loop. There is a noticeable difference between the splines where dynamic fatigue constraints are used, compared to when static loading constraints are used.

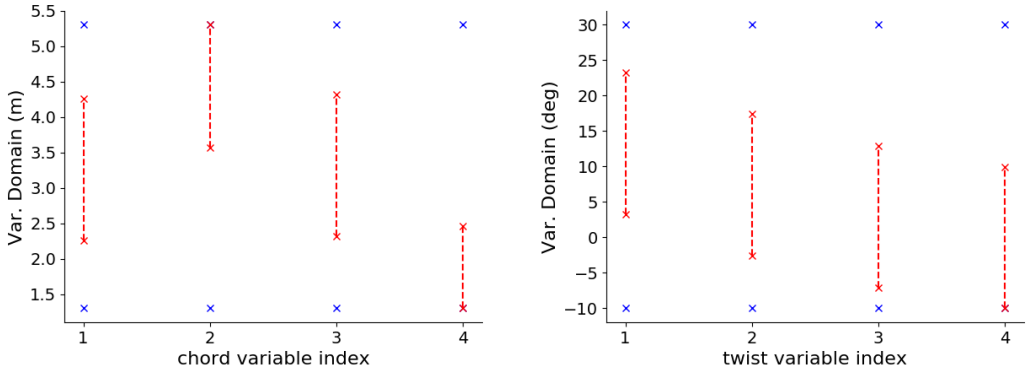

(a) Restricted domain of the chord distribution

(b) Restricted domain of the twist distribution

FIGURE 5 An example of restricting the domain of the chord and twist control points. The blue markers represent the original bounds on the design variables, and the red markers represent the new, more restrictive bounds. Doing this increases the number of points trained where the optimization will likely drive the design.

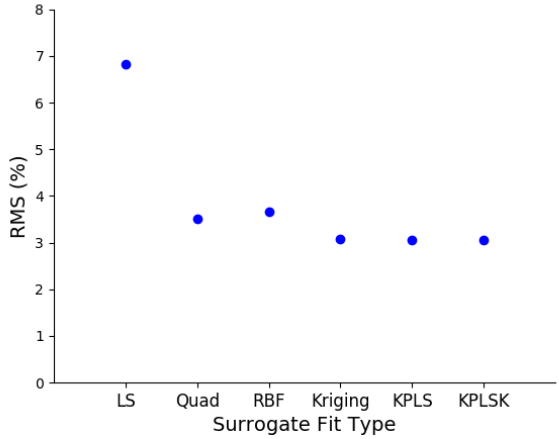

FIGURE 6 The root mean square error using different fits for a 5-fold cross validation.

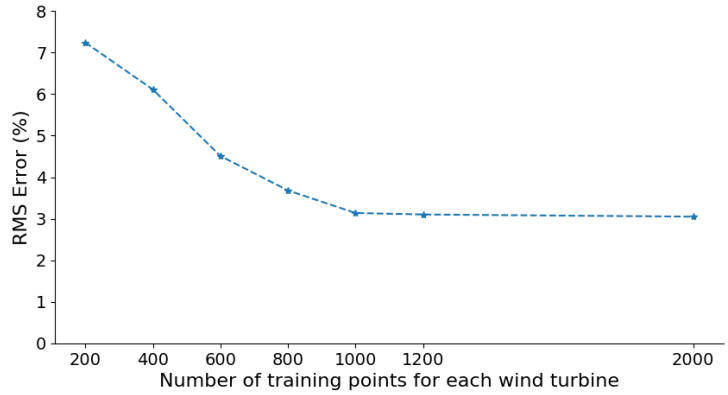

FIGURE 7 The resulting root mean square error from the k-fold cross validation using a Kriging fit for the NREL 5MW reference turbine. There isn't a significant increase in surrogate model accuracy when more than 1000 training points are used for each reference turbine.

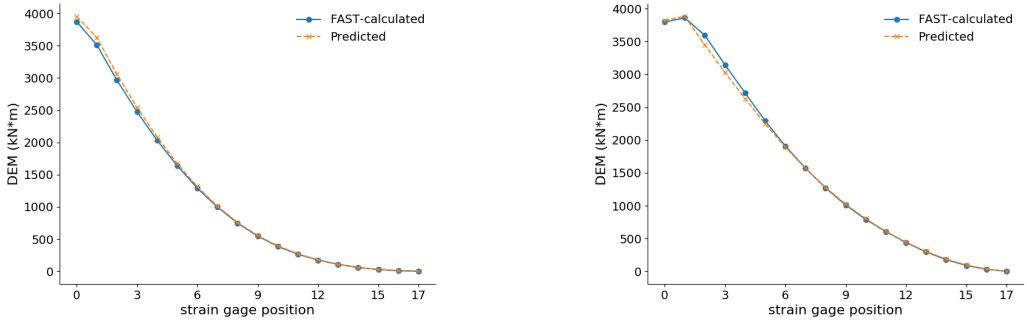

(a) Edgewise DEM

(b) Flapwise DEM

FIGURE 8 The predicted and actual fatigue damage of the 3.0 MW WindPACT reference turbine.

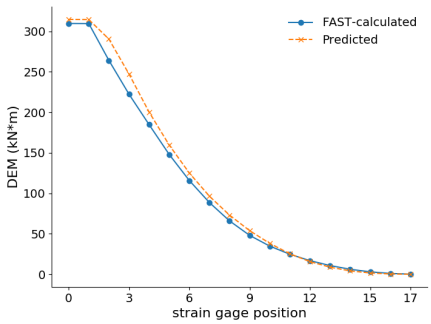

(a) Edgewise DEM

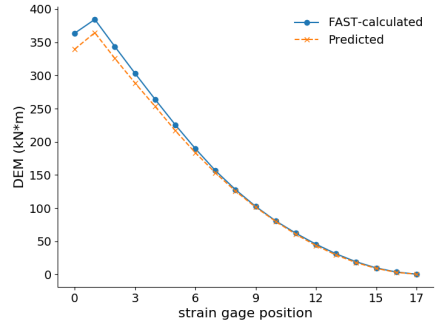

(b) Flapwise DEM

FIGURE 9 The predicted and actual fatigue damage of the 0.75 MW reference turbine.

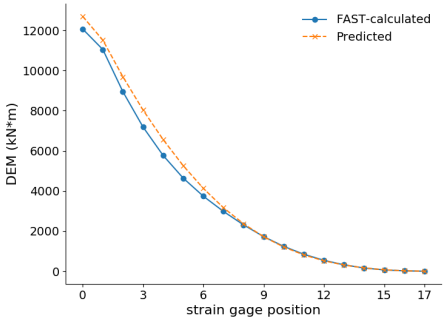

(a) Edgewise DEM

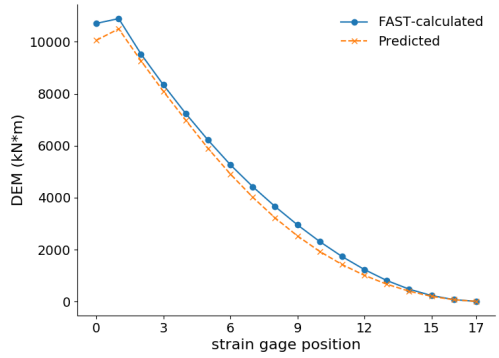

(b) Flapwise DEM

FIGURE 10 The predicted and actual fatigue damage of the NREL 5.0 MW reference turbine.

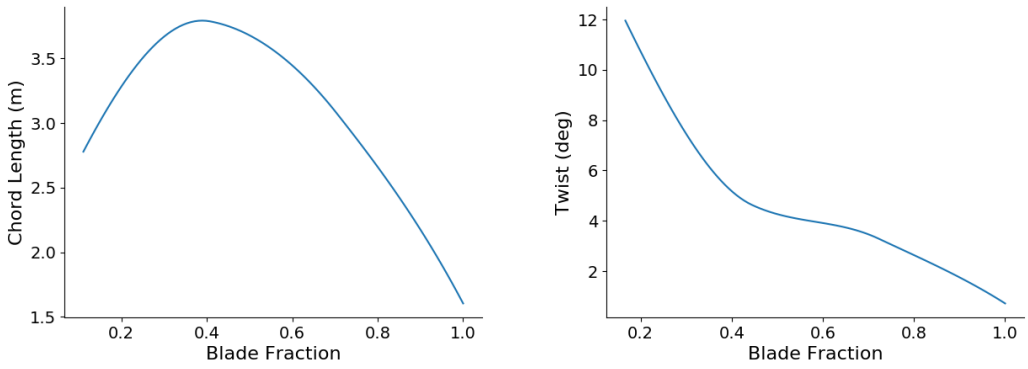

(a) Chord Distribution

(b) Twist Distribution

FIGURE 11 The optimized chord and twist distributions using the surrogate model.